

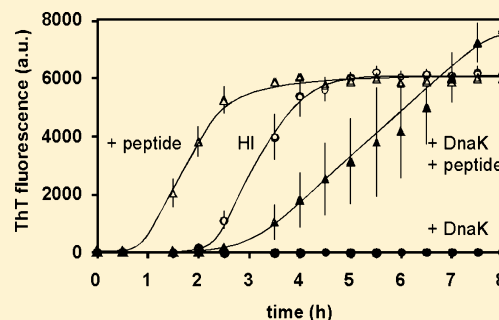
# DnaK Prevents Human Insulin Amyloid Fiber Formation on Hydrophobic Surfaces

Thomas Ballet,<sup>†,‡</sup> Franz Bruckert,<sup>†</sup> Paolo Mangiagalli,<sup>‡</sup> Christophe Bureau,<sup>‡</sup> Laurence Boulangé,<sup>‡,§</sup> Laurent Nault,<sup>†</sup> Thomas Perret,<sup>†</sup> and Marianne Weidenhaupt<sup>\*,†</sup>

<sup>†</sup>Laboratoire des Matériaux et du Génie Physique, Grenoble Institute of Technology, 3 parvis Louis Néel, 38016 Grenoble Cedex 1, France

<sup>‡</sup>Becton-Dickinson Pharmaceutical Systems, 11, Rue Aristide Bergès, 38801 Le Pont de Claix, France

**ABSTRACT:** We have developed a multiwell-based protein aggregation assay to study the kinetics of insulin adsorption and aggregation on hydrophobic surfaces and to investigate the molecular mechanisms involved. Protein–surface interaction progresses in two phases: (1) a lag phase during which proteins adsorb and prefibrillar aggregates form on the material surface and (2) a growth phase during which amyloid fibers form and then are progressively released into solution. We studied the effect of three bacterial chaperones, DnaK, DnaJ, and ClpB, on insulin aggregation kinetics. In the presence of ATP, the simultaneous presence of DnaK, DnaJ, and ClpB allows good protection of insulin against aggregation. In the absence of ATP, DnaK alone is able to prevent insulin aggregation. Furthermore, DnaK binds to insulin adsorbed on hydrophobic surfaces. This process is slowed in the presence of ATP and can be enhanced by the cochaperone DnaJ. The peptide LVEALYL, derived from the insulin B chain, is known to promote fast aggregation in a concentration- and pH-dependent manner in solution. We show that it also shortens the lag phase for insulin aggregation on hydrophobic surfaces. As this peptide is also a known DnaK substrate, our data indicate that the peptide and the chaperone might compete for a common site during the process of insulin aggregation on hydrophobic surfaces.



Adsorption of protein on material surfaces is of widespread importance in fields like cellular biology, pharmacology, and medicine. It can be quantitatively measured either biochemically after desorption or in situ by sensitive biophysical methods, like QCM-D or surface plasmon resonance (SPR). Protein adsorption is accompanied by conformational changes upon contact with the material surface, leading sometimes to protein aggregation. It is not easy to monitor these conformational changes on the material in a fast, convenient, and preferentially multiplexed assay. Albeit greatly sensitive, techniques like attenuated total reflectance Fourier transform infrared spectroscopy (ATR-FTIR) are not readily available and do not provide unambiguous information about the nature of the changes in protein folding.

Within cells, chaperones constitute a set of proteins whose function is to check the folding state of other proteins, and to refold them,<sup>1–3</sup> using ATP hydrolysis energy to drive protein disaggregation and renaturation. In *Escherichia coli*, Bukau and co-workers identified DnaK, DnaJ, and ClpB as the minimum set of bacterial chaperones needed to help the cell recover from a heat shock.<sup>4</sup> DnaK is an ATPase specific for unfolded hydrophobic amino acid stretches. DnaJ forms a complex with DnaK and stimulates DnaK ATPase activity.<sup>5</sup> ClpB is a hexameric ATPase that interacts with aggregated proteins and disaggregates them, in cooperation with DnaK and DnaJ.<sup>4,6,7</sup> Furthermore, in *E. coli*, ~250 proteins are disaggregated and

refolded when DnaK, DnaJ, and ClpB are present, which supports the broadness of their protein substrates.<sup>4</sup> Chaperones detect general conformational unfolding characteristics, rather than specific targets. In addition, many chaperones work in complexes; hence, chaperone combination is likely to enhance the recognition process. We therefore hypothesized that this protein family could provide new sensors for protein conformational changes at material surfaces.

We chose human insulin (HI) as a model because its aggregation has been studied under different physicochemical conditions.<sup>8–10</sup> It was shown that HI aggregation is formulation-dependent and that insulin undoubtedly changes its conformation upon binding to hydrophobic surfaces, leading to the formation and release of amyloid fiber aggregates.<sup>11</sup> From a concentration dependence study, Sluzky et al. deduced that the HI monomer was the molecular species leading to aggregation.<sup>9</sup> Using recombinant chaperones, we observe that different sets of them are able to prevent HI aggregation by binding preferentially to surface-bound insulin. Rüdiger et al.<sup>12</sup> have shown that DnaK binds to the insulin B chain peptide SHLVEALYLVCGER, and Ivanova et al.<sup>13</sup> demonstrated that the shorter LVEALYL peptide is the minimal sequence that can

**Received:** September 19, 2011

**Revised:** January 23, 2012

**Published:** February 21, 2012



accelerate the lag time of insulin fiber formation at acidic pH in a concentration-dependent manner. We show that this same peptide also accelerates the lag time of insulin aggregation on hydrophobic surfaces and that bacterial chaperones are able to counterbalance this effect.

## ■ EXPERIMENTAL PROCEDURES

If not otherwise stated, all chemicals were purchased from Sigma-Aldrich. Experiments were conducted in TBS [25 mM Tris-HCl (pH 7.4) and 125 mM NaCl]. HI (recombinant, expressed in yeast) solutions were prepared at 0.5 mg/mL (86  $\mu$ M). All solutions were filtered (0.22  $\mu$ m) before being used. The LVEALYL peptide was purchased from Genecust (Luxembourg) and dissolved in 20 mM NaOH at a concentration of 4.3 mM.

### Bacterial Chaperone Preparation and Activity Assay.

The bacterial strains used to produce DnaK (Hsp70), ClpB (Hsp100), and DnaJ (Hsp40) were kindly provided by B. Bukau and A. Mogk (Zentrum für Molekulare Biologie Heidelberg, Universität Heidelberg, Heidelberg, Germany). His-tagged ClpB and DnaJ were purified using nickel-nitrilotriacetic acid (Ni-NTA) metal affinity chromatography columns (Qiagen) according to the manufacturer's instructions. DnaK was purified as described by Cegielska and Georgopoulos<sup>14</sup> and McCarty and Walker,<sup>15</sup> with minor modifications by Buchberger et al.<sup>16</sup> The refolding activity of the purified proteins was controlled using the malate dehydrogenase (MDH) renaturation assay.<sup>6,17</sup> The three proteins and ATP were essential for the refolding activity ( $2 \pm 0.3$  nM min<sup>-1</sup> at 1  $\mu$ M DnaK, 0.2  $\mu$ M DnaJ, and 1  $\mu$ M ClpB).

**Insulin Aggregation Assays.** HI aggregation assays were conducted as eight replicates in plastic 96-well microplates. Polystyrene (Greiner Bio-One, contact angle of  $85 \pm 4.7^\circ$ ) or PEO-coated (Corning, contact angle of  $3.5 \pm 5.8^\circ$ ) microplates were used. In fluorescence assays, black polystyrene microplates were used (Nunc Nunclon  $\Delta$  Surface). The plates were covered by plastic sheets, incubated at 37 °C, and shaken at 1200 rpm (Heidolph Titramax, 1.5 mm vibration orbit). At each time point, the solution was pipetted out of the microwells. Part of the solution was filtered to remove aggregated HI (100 nm cutoff). The wells were washed twice with 300  $\mu$ L of TBS. The adsorbed HI fraction was desorbed with 100  $\mu$ L of 5% SDS for a 1 h agitation at 37 °C. Negligible protein material remained on the surface thereafter. The total amounts of HI in solution (nonfiltered), soluble HI, and HI adsorbed in the wells were determined using the bicinchoninic acid (BCA) assay.<sup>18–21</sup> In addition, turbidity ( $\lambda = 600$  nm) or thioflavin T (ThT, 20 or 50  $\mu$ M) fluorescence was directly measured in the wells. Free and bound forms of ThT were measured at a  $\lambda_{\text{ex}}$  of 342 nm and a  $\lambda_{\text{em}}$  of 430 nm and at a  $\lambda_{\text{ex}}$  of 450 nm and a  $\lambda_{\text{em}}$  of 482 nm, respectively,<sup>22</sup> with a 5 nm excitation and emission slit (Tecan Infinite M1000).

**Kinetic Analysis.** The aggregation kinetics proceed in three phases: a lag phase, where the signal was not statistically different from the baseline (mean  $\pm$  standard deviation), a linear growth phase, and a plateau phase. Experimentally, the lag time was defined by the intercept between the linear growth phase and the baseline. The growth rate was defined as the slope of the linear phase and the plateau as the maximal value attained. The parameters were calculated on individual kinetics corresponding to different samples, and the given statistics represent the average and standard deviation for each parameter.

**Protection of Insulin Aggregation by Bacterial Chaperones.** HI aggregation was monitored by turbidity or ThT fluorescence and confirmed by protein quantification after filtration at the end of the experiment. The TBS buffer solution was supplemented with 2 mM MgCl<sub>2</sub> (TBS-M), because Mg<sup>2+</sup> ions are needed for the chaperone ATPase activity. Magnesium itself does not affect HI aggregation. All chaperones were stable in this buffer. The efficiency of chaperone protection was expressed as the lag time before the onset of HI aggregation. As Zn<sup>2+</sup> influences the equilibrium of HI hexamer formation,<sup>23</sup> we tested the effect of Zn<sup>2+</sup> addition (up to 10  $\mu$ M) on HI aggregation: neither HI aggregation kinetics nor DnaK protection was modified.

**Chaperone Binding Assays.** Polystyrene microplates [96 wells, Greiner enzyme-linked immunosorbent assay (ELISA)] were incubated at 37 °C and 1200 rpm with insulin for various amounts of time and blocked with 10 mg/mL bovine serum albumin (BSA) in TBS-M (blocking buffer) for 30 min at room temperature (RT) with shaking (1000 rpm). DnaK, DnaJ, or both (diluted in blocking buffer) were then added for 30 min (RT) with shaking (1000 rpm). The plate was blocked again with BSA for 30 min (RT) with shaking (1000 rpm).

For DnaK detection, a mouse anti-DnaK (*E. coli*) monoclonal antibody (8E2/2; diluted 1:2500 in blocking buffer) was used, and for DnaJ detection, a mouse anti-penta-His antibody (diluted 1:1000 in blocking buffer) was added to each well and the mixture incubated for 15 min (RT) with shaking (1000 rpm). Finally, a goat horseradish peroxidase-conjugated anti-mouse antibody (diluted 1:2500 in blocking buffer) was added to each well and the mixture incubated for 15 min (RT) with shaking (1000 rpm). Wells were then washed three times with 200  $\mu$ L of TBS, and 200  $\mu$ L of ECL substrate solution was added per well. Chemiluminescence signals were immediately recorded using a TriStar LB 941 microplate multimode reader.

To relate luminescence values to the amount of DnaK adsorbed, a calibration experiment was conducted in parallel. Increasing amounts of DnaK were incubated in 96-well polystyrene microplates (Greiner ELISA). The amounts of adsorbed DnaK were determined using the NanoOrange assay, according to the manufacturer's instructions. An ELISA was performed on the adsorbed DnaK as described previously. A calibration curve was then obtained that related luminescence values to the amount of adsorbed DnaK.

## ■ RESULTS

**HI Aggregation in the Presence of Hydrophobic Surfaces.** To study the mechanisms of insulin aggregation on hydrophobic surfaces, we developed a HI aggregation assay using commercial hydrophilic or hydrophobic 96-well plates, to allow rapid screening of different experimental conditions. A HI solution was placed in the presence of hydrophilic or hydrophobic plastic surfaces and agitated at 37 °C. At the indicated times, the solution was recovered and filtered to separate the soluble and aggregated HI pools. The microwell surface was then washed, and adsorbed HI was desorbed with SDS. These three protein pools were then quantified using the BCA assay. In the presence of hydrophilic surfaces, HI remained soluble for several days and less than 1  $\mu$ g of protein was adsorbed on the hydrophilic microwell surfaces (data not shown). In contrast, in the presence of hydrophobic surfaces, the concentration of soluble HI remained constant for  $\sim$ 4 h (lag phase), after which the amount decreased

sharply to trace amounts (Figure 1A). The amount of aggregated HI in solution increased in parallel at a similar rate.

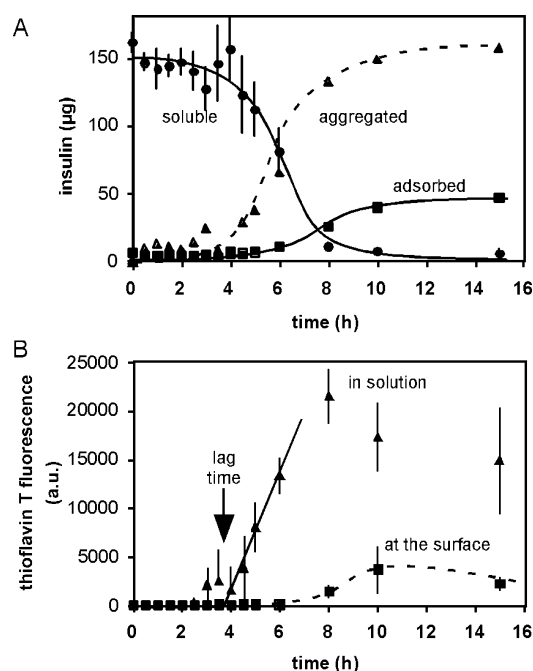


**Figure 1.** Kinetics of human insulin adsorption and aggregation in hydrophobic microplates. (A) Amount of soluble (●), aggregated (▲), and adsorbed (■) HI after the indicated incubation time. (B) Amyloid fiber-bound ThT fluorescence in solution (▲) and on the surface (■) plotted as a function of incubation time. The lag time as the intercept between the growth rate (—) and the baseline is denoted with an arrow. Other curves are hand-drawn and provided as a guide for the eye.

The amount of HI adsorbed on hydrophobic surfaces increased during the aggregation process, reaching a maximum amount of ~40 μg.

Amyloid aggregates are characterized by the formation of intermolecular  $\beta$ -sheets, which can be probed by the binding of thioflavin T (ThT), resulting in a characteristic fluorescence signal. Both the aggregated and the adsorbed HI pools were stained with ThT, and the fluorescence intensity per microgram of protein was the same in both pools (Figure 1B). The ThT fluorescence is therefore a convenient method for monitoring the appearance of HI aggregates. In the following experiments, we defined the lag time as the intercept between the linear growth phase and the baseline of the ThT fluorescence kinetics. Depending on HI preparations, the lag time varied from 2 to 4 h. Within an experiment, using the same HI preparation in the same multiwell plate, the lag time was also variable from well to well, which explains the variation observed in the aggregation kinetics. HI aggregates exhibited elongated fiberlike rods with a diameter of 5–10 nm and a length of 50–100 nm when imaged using electron microscopy (data not shown). Their morphology and dimensions are similar to those of the fibers obtained after incubation of insulin at pH 2 and an elevated temperature.<sup>24,25</sup>

**Effect of Bacterial Chaperones on Insulin Aggregation.** We then studied whether bacterial chaperones could have an effect on the kinetics of HI aggregation. In the presence of 1 mM ATP, the simultaneous presence of the three chaperones delayed HI aggregation as shown by the 9-fold increase in the

aggregation lag time (Figure 2A). DnaK alone slightly increased the lag time, whereas DnaJ was without effect. The combined

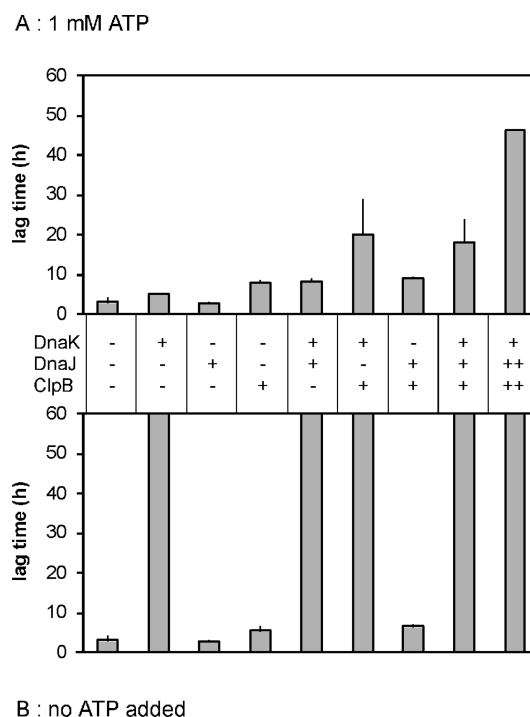


**Figure 2.** Effect of bacterial chaperones on human insulin aggregation. A HI solution was agitated in a hydrophobic microplate, in the presence of DnaK (0.3 μM), DnaJ [0.06 μM (+) and 0.3 μM (++)], and ClpB [0.3 μM (+) and 0.6 μM (++)] as indicated (A) in the presence of 1 mM ATP or (B) in the absence of ATP. The aggregation kinetics were monitored by turbidity, and the lag times were determined as explained in Experimental Procedures.

presence of DnaK and DnaJ significantly increased the lag time, to a level similar to that obtained in the presence of ClpB alone. Moreover, the combined presence of ClpB with DnaK, but not DnaJ, further delayed HI aggregation in the presence of 1 mM ATP. When the concentrations of DnaJ and ClpB were increased (++ vs +), the lag time further increased. These results show that HI undergoes conformational changes during the aggregation process that are recognized and could possibly be repaired by a minimal set of bacterial chaperones. Nevertheless, incubation of 150 μg of final amyloid insulin aggregates with DnaK, DnaJ, and ClpB for 24 h does not allow recovery of more than 1 μg of soluble insulin (data not shown). This suggests that the three chaperones do not dissociate final aggregates but more likely block intermediate aggregation states.

Surprisingly, in the absence of ATP, no protein aggregation was observed whenever DnaK was present (Figure 2B). The effect was specific for DnaK because, in the absence of ATP, the presence of the other chaperones alone or in combination did not significantly change the HI aggregation kinetics. Addition of comparable and larger amounts of BSA, which is routinely used as a blocking agent to cover material surfaces and works by competitive adsorption, had no effect (data not shown). The peculiar role of DnaK is further investigated in the next section.

**Prevention of Insulin Aggregation by DnaK in the Absence of ATP.** In the presence of 1 mM ATPγS, a



nonhydrolyzable form of ATP, DnaK did not prevent HI aggregation (Figure 3A), which showed that no ATP hydrolysis

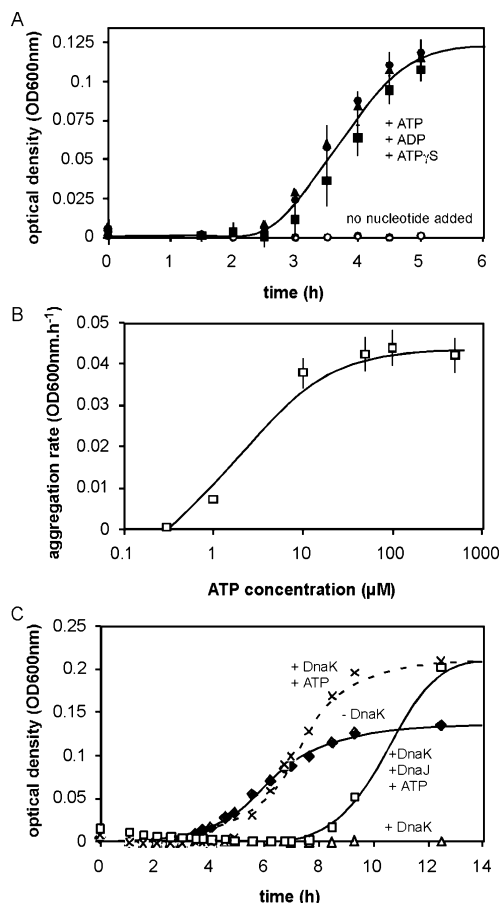


**Figure 3.** Nucleotide requirements for DnaK protection of human insulin aggregation on hydrophobic surfaces. A HI solution was agitated in a hydrophobic microplate in the presence of the indicated chaperones and nucleotides. HI aggregation was monitored by optical density measurements at 600 nm. (A) The HI solution was supplemented with 1  $\mu$ M DnaK and either no nucleotide (○) or 1 mM ATP, ADP, or ATP $\gamma$ S (●, ▲, and ■, respectively). (B) The HI solution was supplemented with 0.3  $\mu$ M DnaK, and the aggregation rate is plotted as a function of ATP concentration. (C) The HI solution was not supplemented with chaperones (◆), supplemented with 0.3  $\mu$ M DnaK in the absence of ATP (△) or with 1 mM ATP (×), or supplemented with 0.3  $\mu$ M DnaK and 0.06  $\mu$ M DnaJ with 1 mM ATP (□).

took place on the HI substrate. Furthermore, addition of 1 mM ADP also abolished the protective effect of DnaK on HI aggregation. The similar effect obtained by the presence of ADP, ATP, or a nonhydrolyzable nucleotide suggested that the molecular species, active at preventing the formation of HI amyloid fibers, was the nucleotide-free DnaK<sub>empty</sub>–HI complex. This fits well with the biochemical properties of this protein because in the presence of ATP, DnaK indeed has a decreased affinity for its protein substrate<sup>26,27</sup> and hence could be less protective against aggregation. A series of HI aggregation experiments were performed in the presence of DnaK at different ATP concentrations ranging from 1  $\mu$ M to 5 mM. The HI aggregation rate was used to measure the effect of added ATP on DnaK (Figure 3B). An apparent affinity of 2  $\mu$ M was determined, which fits with the reported values of the affinity of DnaK for ATP.<sup>28</sup> Furthermore, in the presence of ATP, DnaJ

increased the protective effect of DnaK on HI aggregation (Figure 3C). It is indeed known that the DnaK–DnaJ complex has a higher affinity for the protein substrate than DnaK alone.<sup>29,30</sup>

Several lines of evidence indicate that DnaK prevented early phases of HI aggregation. First, in the continuous presence of DnaK, the amount of HI that adsorbed on hydrophobic surfaces remained small (Figure 4A) and ThT did not stain the adsorbed HI (Figure 4B, vs Figure 1B). Second, in two-stage experiments, when the protective effect of DnaK was released after 5 h by addition of ATP, HI aggregation took place after the same lag time observed in the absence of DnaK (Figure 4C). Similarly, when DnaK was added after incubation for 1 h, the lag time was reduced by 1 h after the addition of ATP. This showed that, as long as it was present in a nucleotide-free form, DnaK prevented the formation of amyloid aggregates on hydrophobic surfaces. To confirm the early effect of DnaK, a constant amount of DnaK was added at different times after the beginning of the incubation. After a 1 h pre-incubation, DnaK considerably slowed HI aggregation kinetics, but after 2 h, it had no significant effect, although aggregation had not yet started (Figure 4D).

#### DnaK Binds to HI Adsorbed on Hydrophobic Surfaces.

We then determined the minimal amount of DnaK that should be added as a function of preincubation time to prevent HI aggregation for at least 18 h (Figure 5). This amount increased very rapidly without exceeding the amount of HI adsorbed on the surface, on a molar ratio basis.

Because insulin aggregates are present both on the plastic surface and in solution, we studied the binding of DnaK to the HI pool adsorbed on the surface and to HI aggregates in suspensions. BCA and sodium dodecyl sulfate–polyacrylamide gel electrophoresis (SDS–PAGE) analysis were combined to quantify the amount of DnaK and HI adsorbed on the surface or to aggregates in suspension (Table 1). For these experiments, we used an experimental setup similar to that of Sluzky et al.<sup>8</sup> SurfaSil-treated borosilicate beads were incubated with HI under agitation overnight. After the beads had been washed, 20  $\pm$  2  $\mu$ g of HI remained adsorbed to the beads. The HI solution fully aggregated, and 150  $\mu$ g of HI aggregates was recovered by centrifugation and washed.

In a first set of experiments, the adsorbed HI pool was incubated with 8  $\mu$ g of DnaK, or buffer alone, in the presence or absence of ATP, for 8 min, and the amount of insulin and DnaK adsorbed on the beads after the incubation was determined. The material released in solution after the incubation was also analyzed by centrifugation, to separate soluble and aggregated proteins, and the amount of DnaK associated with the aggregates was also quantified. In the absence of DnaK, 35% of the initially adsorbed HI detached from the bead surfaces (7  $\mu$ g/20  $\mu$ g), corresponding to the spontaneous detachment of HI aggregates from the surface. In the presence of DnaK, larger amounts of protein, which contained both DnaK and HI, were released from the surface (15.4  $\mu$ g + 2.4  $\mu$ g = 17.8  $\mu$ g). Under these conditions, 77% of the initially adsorbed HI detached from the beads (15.4  $\mu$ g/20  $\mu$ g). This material could be recovered by centrifugation, showing that it contained only HI aggregates. Moreover, an ELISA confirmed that <0.1  $\mu$ g of HI could be recovered in soluble form. No protein renaturation had thus taken place. A large fraction of DnaK (2.4  $\mu$ g of 8  $\mu$ g) cosedimented with the released HI material, and small but significant amounts of DnaK (0.2  $\mu$ g) remained at the bead surface. This strongly suggested that

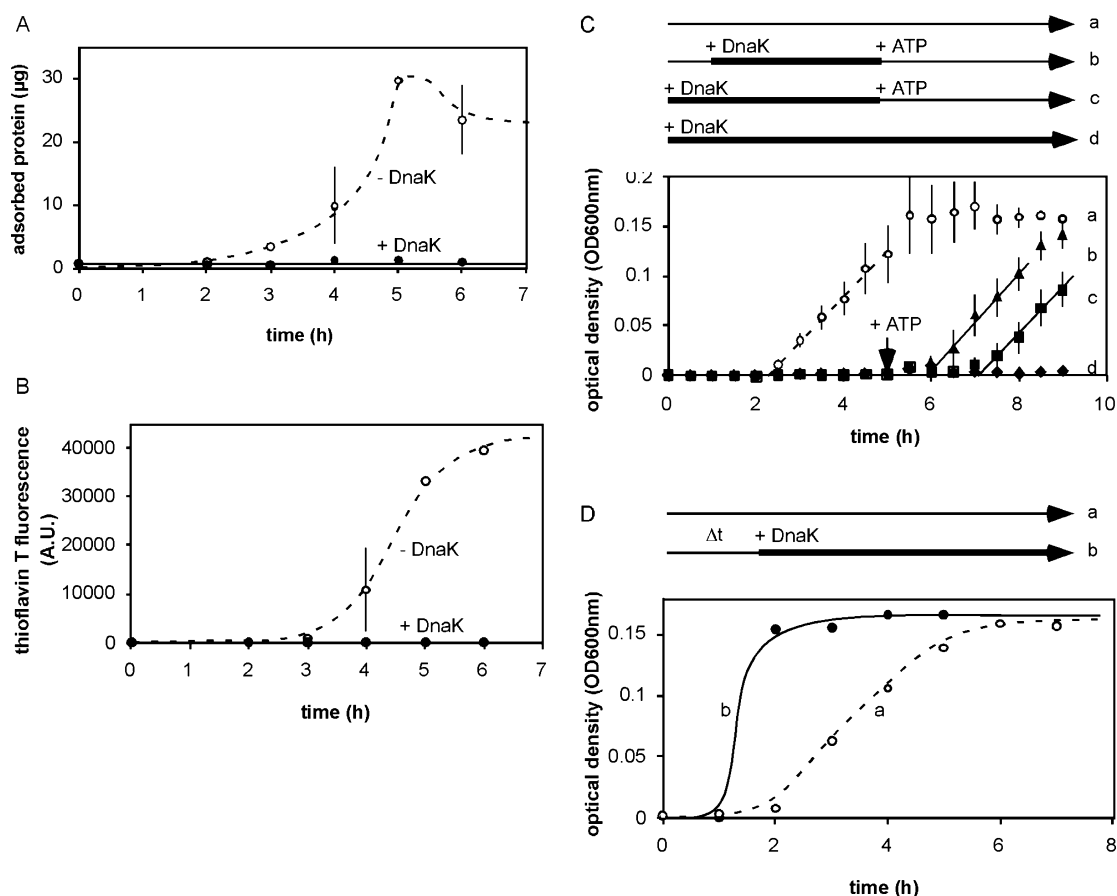


**Figure 4.** DnaK prevents the formation of prefibrillar insulin aggregates on hydrophobic surfaces. (A) Time course of adsorption of HI on hydrophobic surfaces in the presence of 0.3 μM DnaK without ATP (●) compared to the adsorption in the absence of DnaK (○). (B) Time course of amyloid fiber formation on hydrophobic surfaces in the presence of 0.3 μM DnaK without ATP (●) compared to the aggregation in the absence of DnaK (○). (C and D) Two-stage experiments. (C) A HI solution was incubated in the presence (filled symbols, b–d) or absence (○, a) of 0.3 μM DnaK. At the indicated time, 1 mM ATP was added to the DnaK-containing sample (b and c) and the HI solution was further incubated. Bold lines represent the time during which DnaK protects HI from aggregation. HI aggregation was monitored by turbidity. (D) DnaK (0.3 μM) was added at the indicated time (Δt) after the beginning of HI agitation in a hydrophobic microplate, and the incubation was further continued for 8 – Δt hours (●). In comparison, the kinetics of HI aggregation as measured in panel C (a) is shown (○). HI aggregation was monitored by turbidity after 8 h.

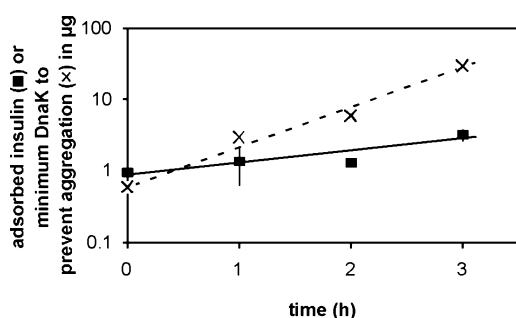


**Figure 5.** Stoichiometry of the interaction of DnaK with insulin adsorbed on hydrophobic surfaces. A HI solution was agitated in hydrophobic microplates for the indicated preincubation time. DnaK was then added at different concentrations, and the HI solution was further incubated for 18 h. The extent of HI aggregation was determined by ThT staining. A 2-fold increase in the level of ThT staining over background was used as a criterion for the onset of HI aggregation. The minimal amount of DnaK needed to prevent the onset of HI aggregation is represented as a function of preincubation time. The amount of adsorbed HI is also represented.

DnaK detached insulin aggregates from the bead surface, remaining associated to them. The time course of this process

was ~20 min (data not shown). In contrast, no DnaK could be detected on hydrophilic surfaces where similar amounts of HI had been preadsorbed (data not shown). Qualitatively similar results were obtained in the presence and absence of ATP. However, less insulin was detached, and ~50% of the DnaK remained bound to insulin aggregates in the presence of 1 mM ATP.

In a second set of experiments, DnaK (8 μg) was incubated with HI aggregates that had already been released in solution. Under these conditions, ~0.5 μg of DnaK was bound to 150 μg of a HI aggregate suspension. This shows that DnaK does not bind efficiently to HI aggregates already present in solution. DnaK therefore binds specifically to HI adsorbed on hydrophobic surfaces.

Making use of the affinity of DnaK for insulin adsorbed on hydrophobic surfaces, we subsequently designed an assay for the sensitive detection of aggregated insulin on material surfaces. Insulin (or BSA as a control) was incubated in the presence of hydrophobic or hydrophilic surfaces for 1 h. The adsorbed protein (1–2 μg) was incubated with increasing amounts of DnaK, in the presence or absence of DnaJ and/or ATP. After the sample had been gently washed, DnaK was detected using anti-DnaK antibodies in a chemoluminescence

**Table 1. DnaK Binding to HI-Covered Surfaces and HI Aggregates and LVEALYL Aggregates in Solution<sup>a</sup>**

	fraction		
	adsorbed	released from beads	
		aggregates	soluble
Hydrophobic Surfaces, No DnaK Added			
human insulin ( $\mu\text{g}$ )	11 $\pm$ 2	7 $\pm$ 3	<0.1
Hydrophobic Surfaces, with DnaK (8 $\mu\text{g}$ )			
human insulin ( $\mu\text{g}$ )	4.6 $\pm$ 1	15.4 $\pm$ 2.5	<0.1
DnaK ( $\mu\text{g}$ )	0.2 $\pm$ 0.1	2.4 $\pm$ 0.6	5.4 $\pm$ 0.7
DnaK:HI molar ratio	277	77	
Hydrophobic Surfaces, with DnaK (8 $\mu\text{g}$ ) and Aggregated Insulin in Solution			
human insulin ( $\mu\text{g}$ )		150 $\pm$ 10	
DnaK ( $\mu\text{g}$ )		0.5 $\pm$ 0.2	
Molar ratio (HI:DnaK)		4200	
Hydrophobic surfaces, with DnaK (1.5 $\mu\text{g}$ )			
LVEALYL ( $\mu\text{g}$ )		25	
DnaK ( $\mu\text{g}$ )		0.5	
Molar ratio (peptide:DnaK)		4000	

<sup>a</sup>Acid-washed borosilicate glass beads (diameter of 1 mm) were siliconized by immersion in SurfaSil (Pierce, 10%, w/w) in acetone and stabilized by being cured at 100 °C for 1 h. The water contact angle was measured (DSA100 Krüss) ( $93.5 \pm 3.5^\circ$ ). SurfaSil-treated beads were incubated with HI in TBS-M buffer overnight. The fully aggregated HI solution was removed, and the beads were washed three times with 500  $\mu\text{L}$  of TBS-M. The initial amount of HI adsorbed on the beads was determined. DnaK was then added, in the presence or absence of ATP, and the beads were further incubated for 1 h at 37 °C under agitation. The total protein content and the amount of HI or DnaK were determined in three fractions: the one adsorbed on the beads, the aggregated one, and the soluble ones released from the beads and separated by centrifugation (5000g for 10 min). The total amount of protein was quantified by the BCA assay; the amount of soluble HI was quantified by an ELISA (I2018 mouse monoclonal anti-insulin antibody), and the amount of DnaK was determined using SDS-PAGE and Coomassie staining. Quantification was performed with ImageJ. For the interaction of DnaK with the aggregated LVEALYL peptide, the peptide solution was prepared at 1 mM glycine buffer (pH 2.5). This solution was incubated in hydrophobic 96-well plates overnight at 37 °C with agitation (1200 rpm). The resulting aggregates were centrifuged and washed three times in TBS-M buffer (pH 7.4) before being resuspended and incubated in TBS-M buffer containing 1.5  $\mu\text{g}$  of DnaK over 30 min. The DnaK/peptide solution was then centrifuged and washed three times in TBS-M buffer before SDS-PAGE analysis.

assay (see Experimental Procedures). In Figure 6A, the amount of adsorbed DnaK is plotted as a function of the total amount of DnaK. In the absence of DnaJ, small but significant amounts of DnaK (26 ng) were bound to insulin adsorbed on hydrophobic surfaces compared to the amount of DnaK bound on adsorbed BSA (14 ng). In contrast, almost no DnaK was recovered when insulin was incubated with hydrophilic surfaces (data not shown). The amount of DnaK bound to adsorbed insulin was only slightly reduced in the presence of 1 mM ATP (23 ng). In the presence of DnaJ, much larger amounts of DnaK were bound to adsorbed HI (372 ng), but not on adsorbed BSA (27 ng). Addition of ATP reduced the amount of DnaK binding in the presence of DnaJ to 147 ng. To study the DnaJ requirement for DnaK binding, the amount of DnaK was kept constant at 2.5  $\mu\text{g}$  (0.18  $\mu\text{M}$ ) and the DnaJ concentration was increased (Figure 6B). DnaK binding reached a maximum for amounts of DnaJ larger than 1.28  $\mu\text{g}$  (0.16  $\mu\text{M}$ ), which corresponds to a 1:1 DnaJ:DnaK ratio. These

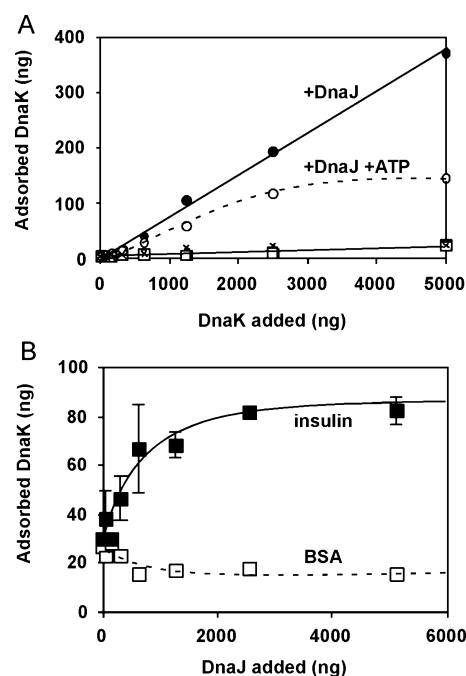


**Figure 6.** Amount of DnaK adsorbed on surface-bound HI. A 0.5 mg/mL insulin or 0.5 mg/mL BSA control solution ( $\times$ ) was agitated for 1 h in a hydrophobic microplate. After removal of the solution, a DnaK solution was added. (A) The DnaK solution was not supplemented with ATP ( $\blacksquare$ ), supplemented with 1 mM ATP ( $\square$ ), and supplemented with DnaJ (0.16  $\mu\text{M}$ ) in the presence of 1 mM ATP ( $\circ$ ) or in the absence of ATP ( $\bullet$ ). The amount of adsorbed DnaK was measured using an ELISA as described in Experimental Procedures and is represented as a function of the total amount of DnaK added. (B) A 0.18  $\mu\text{M}$  DnaK solution supplemented with different amounts of DnaJ was added to the adsorbed insulin ( $\blacksquare$ ) and the adsorbed BSA ( $\square$ ). The amount of adsorbed DnaK was measured using an ELISA as described in Experimental Procedures and is represented as a function of the total amount of DnaJ added. Lines are hand-drawn and provided as a guide for the eye.

data show that DnaK specifically interacts with HI adsorbed on hydrophobic surfaces and that the molecular chaperone DnaJ reinforces this binding. The weak binding of DnaK in the presence of ATP is consistent with its lack of a protective effect against aggregation.

**Competition between the LVEALYL Amyloidogenic Peptide and Bacterial Chaperones during HI Aggregation on Hydrophobic Surfaces.** Recent studies by Ivanova et al.<sup>13</sup> pinpointed the role of two HI amino acid stretches that are likely to change extensively their conformation when HI spontaneously goes from a soluble form to amyloid aggregates at pH 2 and 60 °C. These sequences are SLYQLENY (A12–19) and LVEALYL (B11–17). Both contain hydrophobic residues and are mainly involved in  $\alpha$ -helices in the HI monomer. In amyloid fibers, two LVEALYL stretches from two monomers are assumed to associate into antiparallel extended  $\beta$  sheets that tightly interact via their hydrophobic side chains. The SLYQLENY sequence shows similar properties and also contributes to the formation of fibrillar structures. In this model, the core of HI amyloid fibers is therefore provided by hydrophobic interactions between these polypeptides and stabilized by the stacking of extended  $\beta$ -sheets. To investigate whether hydrophobic surfaces drive similar conformational changes, we studied the effect of the LVEALYL and the SLYQLENY peptides on HI aggregation kinetics. The SLYQLENY peptide

had no effect on HI aggregation kinetics, whereas the LVEALYL peptide strongly reduced the lag time in HI aggregation kinetics at substoichiometric concentrations relative to HI (Figure 7A). At higher concentrations, the

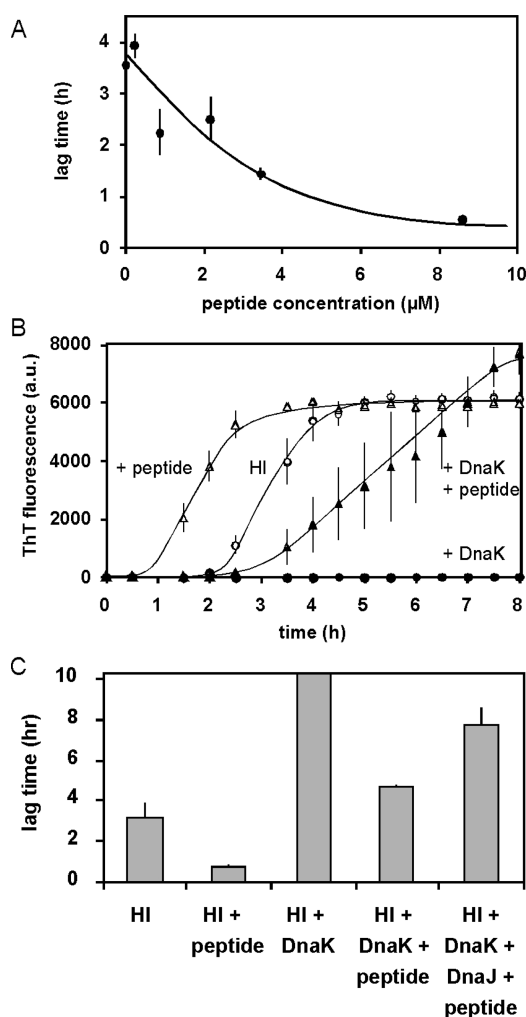


**Figure 7.** Effect of the LVEALYL peptide on HI aggregation kinetics. (A) A HI solution was agitated in a hydrophobic microplate in the presence of different amounts of the LVEALYL peptide, and aggregation was monitored using ThT fluorescence. The lag time (as defined in Experimental Procedures) is represented as a function of peptide concentration. (B) Aggregation kinetics of HI alone (○) or HI supplemented with 26 μM LVEALYL peptide (△), with 0.3 μM DnaK (●), or with both peptide and DnaK (▲). Aggregation was assessed using ThT fluorescence. Lines are hand-drawn and provided as a guide for the eye. (C) A HI solution was agitated in a hydrophobic microplate in the presence of the LVEALYL peptide (8 μM), DnaK (0.3 μM), and DnaJ (0.16 μM), as indicated. Aggregation was monitored using ThT fluorescence, and the lag time was determined. In the presence of DnaK, the lag time extended beyond 10 h.

LVEALYL peptide inhibited the growth of HI amyloid aggregates, as reported previously at pH 2.<sup>13</sup> The effect of the LVEALYL peptide was observed only in the presence of hydrophobic surfaces, the HI solution remaining perfectly stable in hydrophilic multiwell plates, whatever the peptide concentration. It should be noted that none of the peptides alone aggregate in hydrophobic or hydrophilic plates under the same pH, temperature, and concentration conditions.

Rüdiger et al. showed that the SHLVEALYLVCGER and CTSICSLYQLENYCN sequences in insulin bind DnaK.<sup>12</sup> Both encompass the aforementioned peptides involved in amyloid fiber formation (underlined). The same portions of insulin sequence are likely to be recognized by DnaJ, because it shares its substrates with DnaK.<sup>5</sup> It follows that DnaK should antagonize the aggregation promoting effects of the LVEALYL peptide. As shown in Figure 7B, adding 26 μM LVEALYL peptide reduced the HI aggregation lag time from  $2.5 \pm 0.2$  to  $1.1 \pm 0.2$  h. The addition of 0.3 μM DnaK antagonized the effect of the LVEALYL peptide, extending the HI aggregation lag time up to  $4.2 \pm 0.7$  h and slowing aggregation (Figure 7B). The presence of DnaJ enhanced the effect of DnaK [lag time of  $7.8 \pm 0.9$  h (Figure 7C)]. More DnaK was needed to block HI aggregation for longer times. Conversely, ~60 μM LVEALYL peptide was needed to reduce the lag time to the value obtained in the absence of DnaK. Moreover, DnaK binds to amyloid aggregates formed by the LVEALYL peptide alone. Table 1 shows that 0.5 μg of DnaK binds to 25 μg of LVEALYL peptide aggregates.

## DISCUSSION

**DnaK Recognizes a Conformational Change Occurring on HI Adsorbed on Hydrophobic Surfaces.** During aggregation, three pools of insulin were evidenced in this study: the soluble insulin pool, the final amyloid aggregates, and insulin adsorbed on hydrophobic surfaces. In another article, we show that the latter pool contains prefibrillar insulin aggregates that are essential intermediates in the pathway(s) leading to insulin aggregation. The amount of DnaK needed to block insulin aggregation supports the view that DnaK binds to a minor portion of insulin present in the adsorbed insulin pool. The DnaK concentration (0.3–3 μM) is indeed much lower than the HI concentration in solution. Thus, DnaK cannot significantly displace the monomer–dimer–hexamer equilibria and therefore cannot significantly reduce the HI monomer concentration, which is the form of HI in solution that aggregates in the presence of hydrophobic surfaces.<sup>9</sup> Because DnaK weakly interacts with preformed amyloid aggregates released in solution, the binding of DnaK to the end product of the aggregation reaction cannot explain its inhibitory effect (Table 1). The target of DnaK is therefore to be found at the material surface. Because the amount of DnaK needed to block HI aggregation increases during the lag time (Figure 5), we rule out competitive adsorption at the material surface as the reason for DnaK inhibition. Moreover, we show that DnaK directly binds to HI adsorbed on hydrophobic surfaces and to HI aggregates released from the surface (Figure 6 and Table 1). We therefore propose that DnaK blocks the formation of HI amyloid fibers on hydrophobic surfaces, by selective binding to target sequences in adsorbed HI. One of these targets is likely to be the hydrophobic LVEALYL peptide, aggregates of which also bind DnaK (see Table 1 and below).

There is kinetic competition between amyloid fiber growth and protection by DnaK, which is illustrated well by the effect of ATP and DnaJ. ATP-loaded DnaK is known to have a lower affinity for its protein substrate than ADP-loaded DnaK<sup>5</sup> and DnaJ, which stimulates ATP hydrolysis on DnaK and reinforces its interaction with its substrate. Our results suggest that in the absence of nucleotides, DnaK binds strongly to adsorbed HI and DnaJ further stabilizes DnaK binding. When the mean residence time of DnaK on exposed hydrophobic HI stretches is sufficiently long, the formation of amyloid fibers is inhibited



(Figure 4). On the other hand, when the residence time of DnaK is reduced by addition of ATP, aggregates can form rapidly because of the liberation of previously occupied hydrophobic growing fiber ends (Figures 3 and 4). Thus, the absence of ATP, through a substrate affinity increase, allows DnaK to win the competition between adding a blocking DnaK to a growing fiber end and an additional HI molecule, which would promote fiber growth. The competition can also be promoted by a sufficiently high concentration of the LVEALYL peptide, which accelerates HI aggregation so that it overcomes DnaK protection (Figure 7). Although significant amounts of DnaK are released from the surface (Table 1), together with the HI amyloid aggregates, it is the surface-bound DnaK fraction that sets the pace for fiber growth. In the ATP-free state, this latter DnaK fraction exhibits an affinity for growing fiber ends that is sufficiently high to block fiber formation. The inhibitory effect of DnaK on HI aggregation is therefore linked to its presence on the material surfaces.

#### The Amyloidogenic LVEALYL Peptide Is Exposed on HI during Its Aggregation on Hydrophobic Surfaces.

The results of this work and others show that insulin aggregates are able to form and grow on hydrophobic surfaces. What is the likely mechanism of this self-assembly process? Up to 40  $\mu\text{g}$  of HI accumulates on the 2  $\text{cm}^2$  surface area of a single microwell during aggregation (Figure 1A). This high surface concentration (0.2  $\text{g}/\text{m}^2$ ) corresponds to 50 protein layers, assuming a uniform coverage of the surface. A consequence of this observation is that insulin does not merely adsorb on the plain hydrophobic surface, but on insulin already bound to the surface. The effect of the hydrophobic surface should therefore be transmitted from the bottom to the top HI layers, where incoming HI binds. This implies the existence of global conformational changes that relay the effect of the hydrophobic surface. Adsorption of HI molecules on a hydrophobic surface will itself trigger the exposure of a hydrophobic stretch at the surface of adsorbed HI. Although we did not evidence these conformational changes directly, several results support this hypothesis. (i) DnaK binds to HI adsorbed on hydrophobic surfaces, which shows that the structure of the HI protein has changed, exposing one of the two hydrophobic peptides known to bind DnaK: SLYQLENY and LVEALYL. (ii) The LVEALYL peptide itself interacts with HI in the presence of hydrophobic surfaces at a substoichiometric concentration in such a way to accelerate aggregation. This peptide has been shown to form antiparallel  $\beta$ -sheets with itself<sup>13</sup> and could therefore help stabilize a conformational change in insulin by binding to intermediate states. (iii) The antagonist effects of the LVEALYL peptide and DnaK binding on HI aggregation reveal the presence of the same aggregation intermediates in the adsorbed HI pool. (iv) DnaK binds to preformed LVEALYL peptide aggregates. We therefore conclude that the buildup of amyloid fibers on the hydrophobic surface is due to HI adsorption and consequent conformational changes, exposing hydrophobic aggregation-prone sites in the protein. This situation occurs for some proteins, but not all of them. BSA, for instance, strongly binds to hydrophobic surfaces but does not accumulate on them and does not aggregate within an entire week in the presence of hydrophobic surfaces.

**Perspectives.** Our results have interesting potential biochemical and pharmaceutical applications. First, substoichiometric DnaK and DnaJ, in the absence of ATP, could represent a novel and convenient stabilizing additive. Indeed, the low DnaK concentration (0.3  $\mu\text{M}$ ), needed to stabilize HI solutions,

and its selectivity for exposed hydrophobic peptide domains are characteristics that most traditional stabilizing agents lack. Two recent papers by Rasmussen et al.<sup>31,32</sup> showed that the protein  $\alpha$ -crystallin, a member of the small heat shock protein family (sHSP), prevents HI aggregation on hydrophobic surfaces. Molecular chaperones, therefore, represent alternative approaches to guaranteeing the long-term storage of proteins, either in solution or in contact with the container surface. One should nevertheless be aware that DnaK triggers inflammatory responses and thus cannot be injected into patients.<sup>33</sup> DnaK, or better the DnaK–DnaJ combination, could also provide a sensitive in vitro assay to test for protein conformational changes at material surfaces, as shown for HI in this study. By revealing the presence of hydrophobic stretches exposed at the surface of proteins adsorbed on hydrophobic materials, this assay could provide a screening tool for the optimization of protein stability conditions.

#### AUTHOR INFORMATION

##### Corresponding Author

\*Telephone: ++ 33 4 56 52 93 35. Fax: ++ 33 4 56 52 93 01. E-mail: marianne.weidenhaupt@grenoble-inp.fr.

##### Present Address

<sup>§</sup>EIFFAGE Travaux Publics, Centre d'Etudes et de Recherches, 8 rue du Dauphiné, 69960 Corbas, France.

##### Funding

This project was financed by a CNRS "Prise de risques" grant (CHAPROMAT). T.B. is a recipient of a CIFRE fellowship (371/2007). L.N. holds a doctoral fellowship from La Région Rhône-Alpes.

##### Notes

The authors declare no competing financial interest.

#### ACKNOWLEDGMENTS

We thank Benoît Duroux, Frédérique Crozet, and Sébastien Janvier for excellent technical assistance in particle size analysis, Laetitia Rapenne and Isabelle Paintrand in EM analysis and Bernd Bukau, Alexander Mogk, and Matthias Mayer for providing chaperone plasmids and protocols. We are grateful for the scientific input of Yves Bréchet (Grenoble-INP). We thank the CIME facility and BBSI laboratory (CEA Grenoble) for access to their equipment.

#### REFERENCES

- (1) Ellis, R. J., and van der Vies, S. M. (1991) Molecular chaperones. *Annu. Rev. Biochem.* 60, 321–347.
- (2) Ellis, R. J., van der Vies, S. M., and Hemmingsen, S. M. (1989) The molecular chaperone concept. *Biochem. Soc. Symp.* 55, 145–153.
- (3) Ellis, R. J., and Hemmingsen, S. M. (1989) Molecular chaperones: Proteins essential for the biogenesis of some macromolecular structures. *Trends Biochem. Sci.* 14, 339–342.
- (4) Mogk, A., Tomoyasu, T., Goloubinoff, P., Rudiger, S., Roder, D., Langen, H., and Bukau, B. (1999) Identification of thermolabile *Escherichia coli* proteins: Prevention and reversion of aggregation by DnaK and ClpB. *EMBO J.* 18, 6934–6949.
- (5) Bukau, B., and Horwich, A. L. (1998) The Hsp70 and Hsp60 chaperone machines. *Cell* 92, 351–366.
- (6) Goloubinoff, P., Mogk, A., Zvi, A. P., Tomoyasu, T., and Bukau, B. (1999) Sequential mechanism of solubilization and refolding of stable protein aggregates by a bichaperone network. *Proc. Natl. Acad. Sci. U.S.A.* 96, 13732–13737.
- (7) Diamant, S., Ben-Zvi, A. P., Bukau, B., and Goloubinoff, P. (2000) Size-dependent disaggregation of stable protein aggregates by the DnaK chaperone machinery. *J. Biol. Chem.* 275, 21107–21113.



- (8) Sluzky, V., Tamada, J. A., Klivanov, A. M., and Langer, R. (1991) Kinetics of insulin aggregation in aqueous solutions upon agitation in the presence of hydrophobic surfaces. *Proc. Natl. Acad. Sci. U.S.A.* 88, 9377–9381.
- (9) Sluzky, V., Klivanov, A. M., and Langer, R. (1992) Mechanism of insulin aggregation and stabilization in agitated aqueous solutions. *Biotechnol. Bioeng.* 40, 895–903.
- (10) Brange, J., Andersen, L., Laursen, E. D., Meyn, G., and Rasmussen, E. (1997) Toward understanding insulin fibrillation. *J. Pharm. Sci.* 86, 517–525.
- (11) Sharp, J. S., Forrest, J. A., and Jones, R. A. (2002) Surface denaturation and amyloid fibril formation of insulin at model lipid-water interfaces. *Biochemistry* 41, 15810–15819.
- (12) Rüdiger, S., Germeroth, L., Schneider-Mergener, J., and Bukau, B. (1997) Substrate specificity of the DnaK chaperone determined by screening cellulose-bound peptide libraries. *EMBO J* 16, 1507–582.
- (13) Ivanova, M. I., Sievers, S. A., Sawaya, M. R., Wall, J. S., and Eisenberg, D. (2009) Molecular basis for insulin fibril assembly. *Proc. Natl. Acad. Sci. U.S.A.* 106, 18990–18995.
- (14) Cegielska, A., and Georgopoulos, C. (1989) Functional domains of the *Escherichia coli* dnaK heat shock protein as revealed by mutational analysis. *J. Biol. Chem.* 264, 21122–21130.
- (15) McCarty, J. S., and Walker, G. C. (1991) DnaK as a thermometer: Threonine-199 is site of autophosphorylation and is critical for ATPase activity. *Proc. Natl. Acad. Sci. U.S.A.* 88, 9513–9517.
- (16) Buchberger, A., Schroder, H., Buttner, M., Valencia, A., and Bukau, B. (1994) A conserved loop in the ATPase domain of the DnaK chaperone is essential for stable binding of GrpE. *Nat. Struct. Biol.* 1, 95–101.
- (17) Veinger, L., Diamant, S., Buchner, J., and Goloubinoff, P. (1998) The small heat-shock protein IbpB from *Escherichia coli* stabilizes stress-denatured proteins for subsequent refolding by a multi-chaperone network. *J. Biol. Chem.* 273, 11032–11037.
- (18) Olson, B. J., and Markwell, J. (2007) Assays for determination of protein concentration. *Current Protocols in Protein Science*, Chapter 3, Unit 3, 4, Wiley, New York.
- (19) Smith, D. A., and Radford, S. E. (2000) Protein folding: Pulling back the frontiers. *Curr. Biol.* 10, R662–R664.
- (20) Wiechelman, K. J., Braun, R. D., and Fitzpatrick, J. D. (1988) Investigation of the bicinchoninic acid protein assay: Identification of the groups responsible for color formation. *Anal. Biochem.* 175, 231–237.
- (21) Stoscheck, C. M. (1990) Quantitation of protein. *Methods Enzymol.* 182, 50–68.
- (22) LeVine, H. III (1999) Quantification of  $\beta$ -sheet amyloid fibril structures with thioflavin T. *Methods Enzymol.* 309, 274–284.
- (23) Blundell, T. L., Cutfield, J. F., Dodson, G. G., Dodson, E., Hodgkin, D. C., and Mercola, D. (1971) The structure and biology of insulin. *Biochem. J.* 125, 50P–51P.
- (24) Burke, M. J., and Rougvie, M. A. (1972) Cross- $\beta$  protein structures. I. Insulin fibrils. *Biochemistry* 11, 2435–2439.
- (25) Garriques, L. N., Frokjaer, S., Carpenter, J. F., and Brange, J. (2002) The effect of mutations on the structure of insulin fibrils studied by Fourier transform infrared (FTIR) spectroscopy and electron microscopy. *J. Pharm. Sci.* 91, 2473–2480.
- (26) Theyssen, H., Schuster, H. P., Packschies, L., Bukau, B., and Reinstein, J. (1996) The second step of ATP binding to DnaK induces peptide release. *J. Mol. Biol.* 263, 657–670.
- (27) McCarty, J. S., Buchberger, A., Reinstein, J., and Bukau, B. (1995) The role of ATP in the functional cycle of the DnaK chaperone system. *J. Mol. Biol.* 249, 126–137.
- (28) Skowyra, D., and Wickner, S. (1995) GrpE Alters the Affinity of DnaK for ATP and Mg. *J. Biol. Chem.* 270, 26282–26285.
- (29) Suh, W.-C., Burkholder, W. F., Lu, C. Z., Zhao, X., Gottesman, M. E., and Gross, C. A. (1998) Interaction of the Hsp70 molecular chaperone, DnaK, with its cochaperone DnaJ. *Proc. Natl. Acad. Sci. U.S.A.* 95, 15223–15228.
- (30) Liberek, K., Wall, D., and Georgopoulos, C. (1995) The DnaJ chaperone catalytically activates the DnaK chaperone to preferentially bind the sigma 32 heat shock transcriptional regulator. *Proc. Natl. Acad. Sci. U.S.A.* 92, 6224–6228.
- (31) Rasmussen, T., Kasimova, M. R., Jiskoot, W., and van de Weert, M. (2009) The Chaperone-like Protein'-Crystallin Dissociates Insulin Dimers and Hexamers. *Biochemistry* 4893139320.
- (32) Rasmussen, T., Tantipolphan, R., van de Weert, M. and Jiskoot, W. (2010) The molecular chaperone alpha-crystallin as an excipient in an insulin formulation. *Pharm Res* 2713371347.
- (33) Nolan, A., Weiden, M. D., Hoshino, Y., and Gold, J. A. (2004) Cd40 but not CD154 knockout mice have reduced inflammatory response in polymicrobial sepsis: A potential role for *Escherichia coli* heat shock protein 70 in CD40-mediated inflammation in vivo. *Shock* 22, 538–542.